

UC San Diego

UC San Diego Previously Published Works

Title

Viral Receptor-Binding Protein Evolves New Function through Mutations That Cause Trimer Instability and Functional Heterogeneity.

Permalink

<https://escholarship.org/uc/item/83j3t44x>

Journal

Molecular Biology and Evolution, 41(4)

Authors

Strobel, Hannah
Labador, Sweetzel
Basu, Dwaipayan
[et al.](#)

Publication Date


2024-04-02

DOI

10.1093/molbev/msae056

Peer reviewed

Viral Receptor-Binding Protein Evolves New Function through Mutations That Cause Trimer Instability and Functional Heterogeneity

Hannah M. Strobel,¹ Sweetzel D. Labador,¹ Dwaipayan Basu,^{2,3} Mrudula Sane,¹ Kevin D. Corbett ,^{1,3} and Justin R. Meyer^{1,*}

¹School of Biological Sciences, University of California San Diego, La Jolla, CA, USA

²Department of Chemistry and Biochemistry, University of California San Diego, La Jolla, CA, USA

³Department of Cellular and Molecular Medicine, University of California San Diego, La Jolla, CA, USA

*Corresponding author: E-mail: jrmeyer@ucsd.edu.

Associate editor: Deepa Agashe

Abstract

When proteins evolve new activity, a concomitant decrease in stability is often observed because the mutations that confer new activity can destabilize the native fold. In the conventional model of protein evolution, reduced stability is considered a purely deleterious cost of molecular innovation because unstable proteins are prone to aggregation and are sensitive to environmental stressors. However, recent work has revealed that nonnative, often unstable protein conformations play an important role in mediating evolutionary transitions, raising the question of whether instability can itself potentiate the evolution of new activity. We explored this question in a bacteriophage receptor-binding protein during host-range evolution. We studied the properties of the receptor-binding protein of bacteriophage λ before and after host-range evolution and demonstrated that the evolved protein is relatively unstable and may exist in multiple conformations with unique receptor preferences. Through a combination of structural modeling and in vitro oligomeric state analysis, we found that the instability arises from mutations that interfere with trimer formation. This study raises the intriguing possibility that protein instability might play a previously unrecognized role in mediating host-range expansions in viruses.

Key words: novelty, protein evolution, bacteriophage, nongenetic heterogeneity, experimental evolution, receptor-binding protein.

Introduction

The evolution of new phenotypes at the organismal level can often be traced to functional innovation in a protein. In viruses, for example, changes in proteins that mediate host attachment may confer an expanded host range (Tétart et al. 1996; Yehl et al. 2019; Boon et al. 2020). It is commonly observed across diverse protein types that functional innovations come with a concomitant decrease in stability (Wang et al. 2002; Studer et al. 2014). The most accepted explanation for this is that decreased stability is a deleterious side effect of mutations that generate innovations (Bloom et al. 2006), and compensatory stabilizing mutations ameliorate the cost (Wang et al. 2002; Tokuriki et al. 2008). An alternative hypothesis is that instability is not simply a side effect of innovation but instead contributes to its emergence by facilitating the ability of a single amino acid sequence to sample multiple folds, potentially fueling faster innovation (Tokuriki and

Tawfik 2009; Sikosek and Chan 2014; Dellus-Gur et al. 2015).

The relationship between stability and the evolution of new functions has been understudied in virus receptor-binding proteins (RBPs) compared to enzymes. A study on *vesicular stomatitis virus* showed that genetic robustness, a trait correlated with stability, did not enhance the ability of viruses to adapt to a new host, but the study did not explore a molecular mechanism (Cuevas et al. 2009). A separate study on bacteriophage λ revealed that mutations in its RBP (protein J) confer the use of a new receptor (Meyer et al. 2012) also destabilize the viral particle (Petrie et al. 2018), but instead of simply causing generic misfolding, the instability was thought to alter the folding landscape of J such that sometimes the peptide sequence stochastically folded into an alternative, less-stable conformation. Three lines of evidence were uncovered suggesting that evolved λ s also exhibited this type of nongenetic phenotypic heterogeneity. First, the decay

Received: February 14, 2023. **Revised:** February 07, 2024. **Accepted:** March 11, 2024

© The Author(s) 2024. Published by Oxford University Press on behalf of Society for Molecular Biology and Evolution.

This is an Open Access article distributed under the terms of the Creative Commons Attribution-NonCommercial License (<https://creativecommons.org/licenses/by-nc/4.0/>), which permits non-commercial re-use, distribution, and reproduction in any medium, provided the original work is properly cited. For commercial re-use, please contact reprints@oup.com for reprints and translation rights for reprints. All other permissions can be obtained through our RightsLink service via the Permissions link on the article page on our site—for further information please contact journals.permissions@oup.com.

Open Access

rate of the evolved λ genotype decreased with time, a pattern that would be expected for a phenotypically mixed population (Russell 2021). Second, when evolved λ particles were incubated without host bacteria to replicate on, infectivity on the new receptor, OmpF, declined more rapidly than infectivity on the native receptor, LamB, suggesting the presence of an unstable subpopulation of OmpF-using particles. Third, it was shown that the subpopulation of OmpF-binding particles could be removed from stocks of evolved λ particles by incubation with cells only expressing OmpF, leaving behind particles that preferentially bound LamB. All three results would be abnormal for an isogenic phage stock and were instead consistent with phenotypic heterogeneity. The observation that it was the unstable phenotype that appeared to preferentially interact with OmpF suggests that destabilizing the native fold was necessary to produce the OmpF-binding conformation.

In a follow-up study to the 2018 λ study, it was shown that the stability of the RBP did not decrease coincidentally with the gain-of-function mutations. Instead, destabilization of the RBP was necessary for the gain-of-function mutations to confer activity on OmpF. Populations of thermostable λ genotypes evolved alongside unmodified genotypes required destabilizing mutations to evolve prior to the gain-of-function mutation in order to gain activity on OmpF (Strobel et al. 2022). The counterintuitive result that a thermostable variant had less evolutionary potential, or lower evolvability, than an unstable variant suggests that the ability to generate unique phenotypes can outweigh the costs of instability.

In the 2018 and 2022 λ studies, all experiments were conducted using whole phage particles, and since the ancestor genotype and the evolved genotype differed only by amino acid substitutions in the C-terminal region of the RBP (J), it was inferred that conformational heterogeneity in the J protein was the cause of phenotypic heterogeneity in the evolved λ s (Petrie et al. 2018). This inference seems reasonable, but it is also possible that the heterogeneity could arise due to interactions between J and other λ proteins and structures. To establish better support for the hypothesis that heterogeneity in λ had an evolutionary benefit of expanding the conformational repertoire of J, we measured three functional properties of the purified reactive domain of J before and after evolving to use OmpF.

The first step was to establish a robust protocol for purifying the reactive region of J. This posed a significant challenge because previous attempts to purify the J protein encountered difficulties with expression of even the wild-type protein and relied on fusing the C-terminal J domain to maltose-binding protein (MBP) in order to achieve sufficient solubility for purification (Wang et al. 1998, 2000; Berkane et al. 2006). Purification of the evolved OmpF⁺ version had never been attempted. We developed a protocol to purify the reactive domain of the wild-type and evolved OmpF⁺ J without MBP, an achievement that allowed more sensitive biochemical assays without interference from the fused MBP molecule. Having successfully

purified both wild-type and evolved proteins, we employed a thermal shift assay to measure temperature-mediated unfolding. The assay revealed striking differences in baseline foldedness and melting temperature between the wild-type and evolved proteins, suggesting that the evolved protein is unstable. Next, we tested the hypothesis that the instability originates, at least in part, from mutations that interfere with J-trimer formation. Three J monomers associate with one another at the distal end of the phage tail and one J mutation occurs within residues that are responsible for trimer formation. Using purified proteins, we further found that evolved J was much less likely to form stable trimers than the ancestral J protein. Lastly, seeking a functional link between conformational heterogeneity and the new activity of the evolved protein on OmpF, we tested the hypothesis that an isogenic population of evolved J proteins is composed of at least two subpopulations: one stable, LamB-preferring and one unstable, OmpF-preferring. Indeed, we found that a mild heat treatment reduced activity on OmpF but did not affect activity on LamB, consistent with the existence of uniquely folded forms.

Results

A Protocol for Purifying the Reactive J Domain without MBP

Previous efforts to purify the J protein have used two approaches. The first attempt to purify the full-length J (1,132 amino acids) resulted in an insoluble, aggregated form that required treatment with the surfactant sarkosyl to improve solubility (Wang et al. 1998). A second attempt created multiple constructs by fusing the C-terminal 249, 349, and 449 residues of J to MBP, a protein that acts both as an affinity tag and improves the solubility of its fusion partner (Wang et al. 2000). This allowed expression and purification without using chemical solubilization, and the resulting protein was active on the LamB receptor (Berkane et al. 2006). Seeking to improve on these pioneering efforts to increase solubility and yield, we generated a double-tagged construct containing the C-terminal 249 amino acids of J, MBP, and a hexahistidine (His₆) tag to enable purification using nickel affinity chromatography (Nallamsetty et al. 2005). Although the double-tagging strategy yielded highly pure, active protein suitable for some assays, the large MBP tag rendered these constructs useless for a thermal shift assay because MBP is itself a protein that interacts with the fluorescent dye, obscuring the signal from the smaller J domain. Therefore, we sought to develop a strategy to purify MBP-free J domain for the thermal shift assay. During the course of this study, the revolutionary structural prediction tool AlphaFold (Jumper et al. 2021) became publicly available (Mirdita et al. 2022), and examining the predicted J protein structure yielded a clue as to how we might increase the solubility of the J domain without MBP. We observed that the C-terminal truncation (249 amino acids) consisted

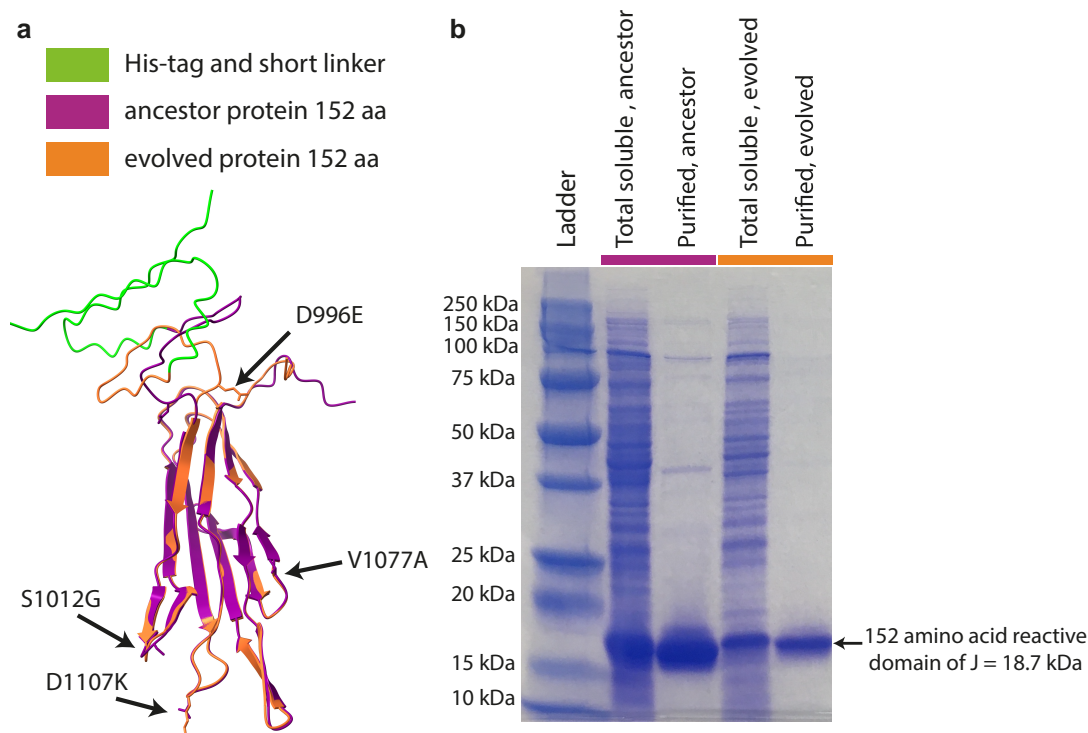


Fig. 1. Despite nearly identical AlphaFold predicted structures, the evolved protein appears less soluble. a) Aligned AlphaFold modeled structures of ancestor J (fuchsia) and evolved J (orange). Models correspond to the 152 C-terminal amino acids of the full 1132 amino acid J protein. Each was purified using a His₆-tag attached N-terminally via a short linker sequence (green). The four amino acid changes that confer OmpF recognition are indicated. b) SDS-PAGE gel showing that the evolved J produces lower soluble and purified yield than the ancestor.

primarily of a region of structurally ordered beta sheets, except for an initial stretch of apparent disorder. We hypothesized that an even shorter truncation that excluded this initial region might increase solubility. Indeed, when we expressed only the C-terminal 152 amino acids of J, along with a His₆-tag (His₆-J⁹⁸¹⁻¹¹³²; Fig. 1a), we obtained soluble protein for both the wild-type and evolved OmpF⁺ genotypes without the MBP tag (Fig. 1b).

Assessing Stability of the Wild-Type and Evolved J Domains

With the purified reactive J domains, we then sought to test the hypothesis that the observed heterogeneity in evolved λ s was caused by instability and conformational heterogeneity in the reactive J domain. We employed a thermal shift assay (Crowther et al. 2010; Huynh and Partch 2015) where purified proteins are mixed with SYPRO Orange, a fluorescent dye that binds hydrophobic residues, which are buried within the core of proteins in the folded state but become exposed during unfolding. The temperature is slowly increased, and fluorescence is measured at 0.5 °C increments. The fluorescent signal for an initially well-folded protein resembles a sigmoidal curve, remaining low until the temperature reaches the melting point, and then the signal rapidly rises as the hydrophobic core unfolds (Crowther et al. 2010; Huynh and Partch 2015). By first examining the initial fluorescence, we observed that the signal from the evolved J domain was

substantially higher than the initial fluorescence of the wild-type domain (Fig. 2a). This suggests that some fraction of the molecules are unfolded at the starting temperature of the assay, 25 °C (Crowther et al. 2010), or that the protein is more dynamic allowing the dye to penetrate the hydrophobic core as would be expected for an unstable protein. Beyond the difference in initial fluorescence, there was also a shift in the melting temperature, calculated as the temperature at which the maximum first derivative of fluorescence occurred (Huynh and Partch 2015). The wild-type J domain's melting temperature was about 20 °C higher than that of the evolved J domain (Fig. 2b). There are several phenomena that could explain the dramatic difference in melting temperature. One possibility is that some fraction of the evolved proteins begin the assay folded but melt at a lower temperature than the wild-type proteins. Another possibility is that most of the evolved proteins begin the assay in an unfolded, aggregated state, and the melting peak is observed when the aggregate melts. We did not probe this result further, and this conundrum has been previously cited as a limitation of the thermal shift assay (Crowther et al. 2010). Both outcomes would suggest that the evolved J domain is unstable relative to the ancestral, which is consistent with experiments on whole phage particles.

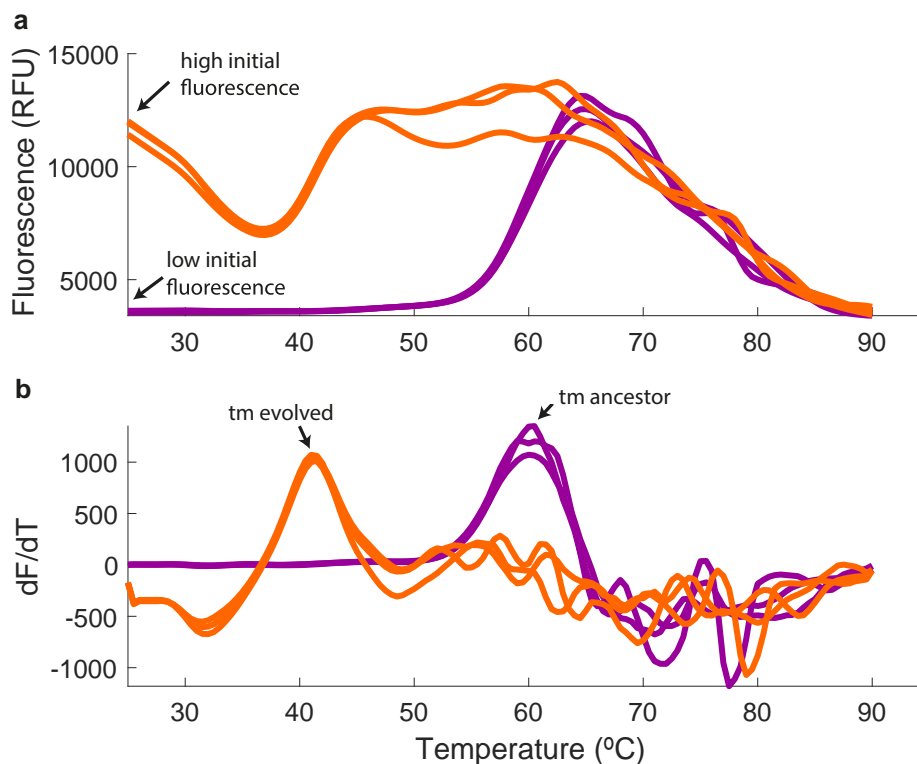


Fig. 2. In a thermal shift assay, the evolved His6-J^{981–1132} has a higher initial fluorescence and lower melting point than the ancestor. a) Melting curves for three replicates of each protein variant revealed substantially higher initial fluorescence for the evolved J compared to the ancestor. This indicates that a fraction of the evolved proteins have exposed hydrophobic residues even at 25 °C, the starting temperature of the assay. b) The first derivative of the melting curve revealed that the evolved J also has a lower melting point than the ancestor, as indicated by the shift in the peaks. Fuchsia curve, ancestor; orange curve, evolved. Tm for three replicates of ancestor: 60 °C, 59 °C, and 60.5 °C. Tm for three replicates of evolved: 41 °C, 41.5 °C, and 41 °C (tstat = 39.598, df = 5, $P = 2.4 \times 10^{-6}$).

Testing One Source of the Instability: Trimer Formation Interference

Upon further inspection of the predicted J structure and the location of J mutations, we developed a new hypothesis for how J instability arises. Most of the mutations occur in loops at the end of the protein that is thought to interact directly with the receptors. However, D996E occurs in what appeared to be a disordered region at the N-terminal sequence (Fig. 1). Despite appearing disordered, this stretch of the protein was predicted with high confidence, suggesting it was not disordered and was part of a larger structure. We hypothesized that this region may be involved in trimer formation and that the mutation could create instability by interfering with quaternary structure. To test this, we used AlphaFold to predict the structure of a trimer of the C-terminal domains of J (residues 615 to 1132). This region comprises several individual domains, including two fibronectin domains, an alpha-helical shaft (AHS), a central straight fiber (CSF) domain with a trimeric beta-helix fold, and the C-terminal receptor-binding domain (RBD). Within the fibronectin and AHS domains (residues 615 to 862), our model agrees closely with a recent cryoelectron microscopy structure of the λ tail complex (2.3 Å r.m.s.d. across 188 aligned C α atoms) (Wong et al.

2024). The C-terminal CSF and RBD domains were not visualized in that structure due to flexibility, but our structure prediction is nonetheless highly confident in these domains. We found that D996 is positioned at the interface of the CSF and RBD domains and is predicted to form a hydrogen bond with the backbone amide group of residue L1127 (Fig. 3). Based on the predicted structure, mutation of D996 to a larger residue (glutamate; E) is expected to cause a steric clash or otherwise disrupt this interaction. Given that the extreme C-terminal five residues of J (residues 1128 to 1132) are predicted to form a short beta-strand that interacts with the neighboring RBD, the disruption caused by the D996E mutation may destabilize this RBD–RBD interaction. Further supporting the functional interaction between residues 996 and 1127 is that in multiple λ evolution experiments where the phage evolved to use OmpF, L1127 mutated on the path to gaining the new function (Meyer et al. 2012).

We tested whether the evolved version of J (which contains the D996E mutation) is less likely to form trimers than the ancestral version. To do this, we analyzed the oligomeric state of MBP-tagged versions of the ancestral and evolved versions of J^{981–1132}, which contains only the RBD and a short stretch of the CSF domain, and whose oligomeric state is therefore expected to depend heavily

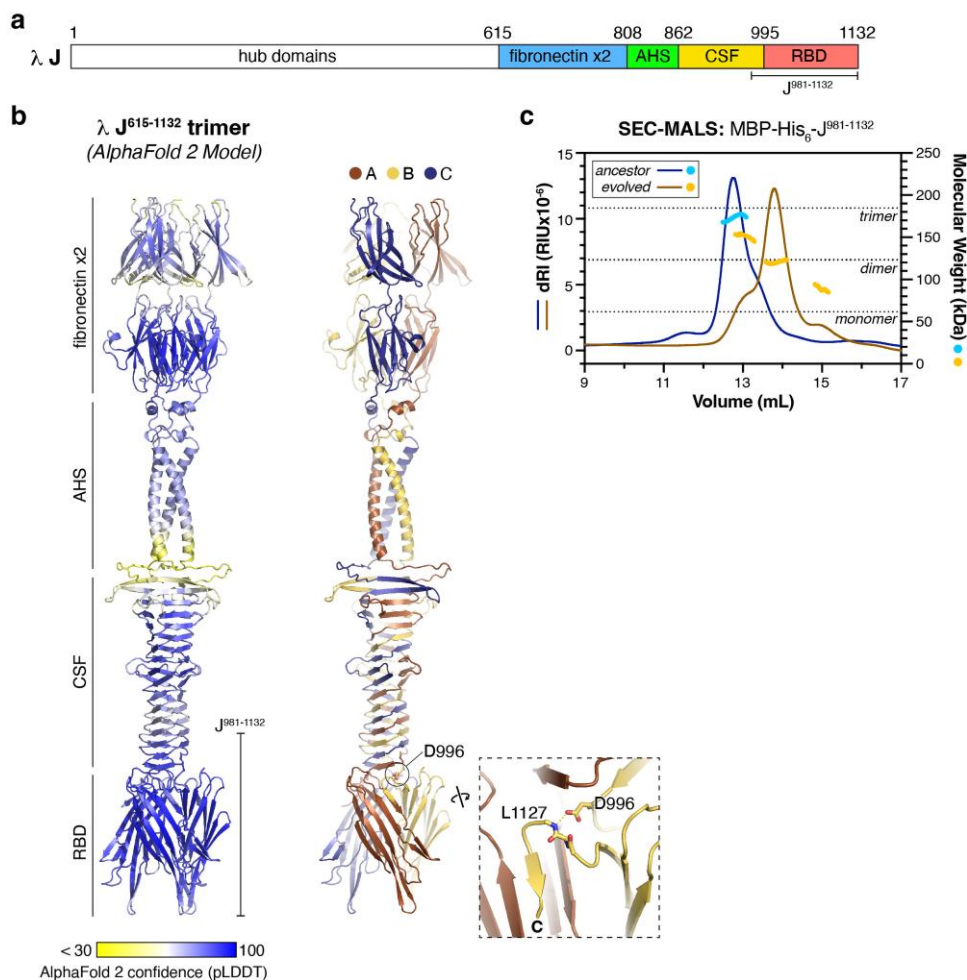


Fig. 3. Structure predictions of a J trimer reveal a tightly interwound architecture with the RBD positioned at the end of the tail. Amino acid substitution D996E occurs at the interface of the CSF domain and the RBD. Panel a) provides a linear structural map of the protein and Panel b) the AlphaFold structure prediction beyond the hub domains (structure prediction of the hub domains was unreliable). Left image shows AlphaFold confidence per-residue model confidence score (pLDDT score), colored from yellow indicating low confidence to blue indicating high confidence). Right image shows the same structure with the three monomers colored brown, yellow, and blue. Inset shows the predicted hydrogen-bonding interaction between D996 and the backbone amide of L1127. c) SEC-MALS analysis of the ancestor and evolved MBP-His6-J⁹⁸¹⁻¹¹³² construct. The ancestral version (blue/light blue) primarily forms trimers, while the evolved version (brown/yellow) forms a range of oligomeric states. Expected molecular weights for His6-MBP-J⁹⁸¹⁻¹¹³² monomer (61.6 kDa), dimer (123.2 kDa), and trimer (184.7 kDa) are indicated by dotted lines. Measured molecular weight for ancestor (trimer peak): 173.4 kDa. Measured molecular weight for evolved: 150.9 kDa (first shoulder), 120.4 kDa (main peak), and 89.1 kDa (last shoulder).

on RBD–RBD interactions. We analyzed MBP-tagged versions of J⁹⁸¹⁻¹¹³² using size exclusion chromatography coupled to multiangle light scattering (SEC-MALS). The MBP-tagged version was used to purify larger quantities of the proteins required for SEC-MALS. MBP is not known to form trimers and the linker was significantly long so we predicted that this tag would not affect trimer formation. Indeed, the ancestor readily formed trimers as evidenced by the elution profile where most of the protein has a molecular weight equal to trimers of the construct, with a minor peak representing a dimer (Fig. 3). The evolved version was much less likely to form trimers, instead showing a mixture of oligomeric states including monomer, dimer, and trimer (Fig. 3). These observations provide evidence that the J mutations decrease the stability of self-association within the J RBD. While the domains N-terminal to residues 981 to 1132 are likely to mediate

stable trimer formation in the context of the full-length protein, we hypothesize that the functional heterogeneity evolves through mutation that creates disorder and/or disrupts the stability of the self-associated J RBDs, which may, in turn, enable flexibility in these domains' ability to recognize diverse cellular receptors.

Assessing Heterogeneity in the Wild-Type and Evolved J Domains

We then designed a test for conformational heterogeneity in the evolved J domain that would shed light on the relationship between nonnative conformations of the J domains and their OmpF activity. In whole phage experiments, it was shown that populations of evolved λ lost infectivity on cells expressing OmpF faster than on cells expressing LamB suggested the OmpF-binding

phenotype may be less stable (Petrie et al. 2018). To test whether this was the case for the purified J domains as well, we designed a treatment that would selectively remove the least stable J molecules and measured the ability to bind LamB and OmpF receptors before and after treatment. For this assay, we used the double-tagged constructs because they produced higher yields in purification. As expected, the wild-type proteins had robust activity on LamB and completely lacked activity on OmpF, and that was unchanged by the heat treatment (Fig. 4a and b). The evolved proteins, on the other hand, lost the ability to bind OmpF faster than they lost the ability to bind LamB (Fig. 4b and c), consistent with the hypothesis that the unstable J conformations are responsible for OmpF binding. Unexpectedly, there was a slight gain in LamB binding after the heat treatment (Fig. 4b and c). We did not delve further into this finding, but we suspect that the heat treatment could have increased thermal energy and allowed some unstable OmpF conformers to refold into stable LamB conformers or perhaps the different conformations might interfere with each other's binding and removing a subset of conformations by heat treatment might have improved the remaining conformation's ability to bind. Together, these results are consistent with the model that evolved λ s contain J proteins of different conformations, and this heterogeneity allowed evolved λ s to use OmpF as a receptor.

Discussion

Instability is generally considered a cost of protein adaptation. We presented evidence that in some cases, protein instability potentiates adaptation by facilitating heterogeneity. A prior study on bacteriophage λ demonstrated instability and phenotypic heterogeneity among particles that had evolved to use a new receptor, OmpF. In this study, we narrowed our focus to just the reactive domain of the λ RBP (J) to evaluate whether conformational heterogeneity in J could have caused the phenotypic heterogeneity in the whole particle, thereby potentiating the evolution of OmpF use. We purified wild-type and evolved J domains and measured their baseline foldedness, melting temperature, trimer association potential, and conformational heterogeneity. Consistent with our hypothesis, the evolved J domains exhibited a higher initial fluorescence when treated with a dye that binds hydrophobic residues, suggesting a higher fraction of unfolded protein even before heat treatment and the melting temperature of the evolved version was ~ 20 °C lower than the wild type. Protein modeling coupled with trimer association assays revealed that the evolved J was less likely to form trimers, creating a likely source of protein instability and functional heterogeneity. Lastly, a functional assay demonstrated that evolved J domains lose activity on the new receptor, OmpF, after heat treatment but retain full activity on the native receptor, LamB, providing evidence of conformational heterogeneity. The protein instability and heterogeneity appear to arise, at least in

part, due to mutations interfering with the self-association of the C-terminal domain of J. Our results corroborate a model in which destabilizing mutations alter J such that it produces a new conformational subpopulation with activity on OmpF, conferring an expanded host range (Petrie et al. 2018).

As structural techniques become more sensitive, it is becoming apparent that structural heterogeneity is not uncommon among proteins (Madhurima et al. 2021). The most common examples are intrinsically disordered proteins, which lack a defined three-dimensional structure, (Oldfield and Dunker 2014), allosteric enzymes, which undergo conformational rearrangements upon binding a ligand (Beveridge et al. 2016), and prions (Li et al. 2009). Another class, known as metamorphic proteins, can access multiple folded conformations from a single peptide sequence, and their conformational state is not determined by binding (Dishman and Volkman 2018). Examples of metamorphic proteins span diverse protein types, from enzymes (Chang et al. 2015) to signaling proteins (Tuinstra et al. 2008) to scaffold proteins (Markley et al. 2013). In many animal viruses, glycoproteins that mediate membrane fusion in often undergo a pH-induced conformational change (Carr and Kim 1993; Roche et al. 2007). Metamorphic proteins typically interconvert between states, but there is considerable variation in time-scale (Luo and Yu 2008; Tuinstra et al. 2008; Markley et al. 2013; Chang et al. 2015), and some may not interconvert at all due to a high energetic barrier between structures (Sinclair et al. 2022). In the case of the evolved λ J domain, our ability to separate conformational subpopulations with pull-down experiments suggests that interconversion between conformations is slow or nonexistent.

In addition to being structural curiosities, metamorphic proteins are also thought to play important roles in evolutionary transitions (Madhurima et al. 2021). By adopting multiple structures, a metamorphic protein can act as a bridge between the current and new functions (Sikosek and Chan 2014). In a study on synthetic small proteins, fold-switching sequences facilitated the formation of diverse multimeric structures with new binding activities (Yadid et al. 2010). In λ , the generalist J protein domain used in this study may represent an evolutionary bridge between a LamB-reliant ancestor and an OmpF specialist. If the metamorphic property of the evolved J domain is in fact related to instability, it might then be expected that mutations that optimize the new function on OmpF might restabilize J (Sikosek and Chan 2014). Indeed, prior work demonstrated this result in whole λ particles (Meyer et al. 2016; Petrie et al. 2018), and it will be informative to test this hypothesis with the purified J domains from OmpF specialists.

The idea that nongenetic phenotypic variation could be a mechanism by which organisms bridge evolutionary transitions is not a new idea, although the more common view is that only genetic variation provides the fuel for evolutionary novelty. In 1953, Waddington observed that a new wing phenotype in fruit flies (*Drosophila melanogaster*),

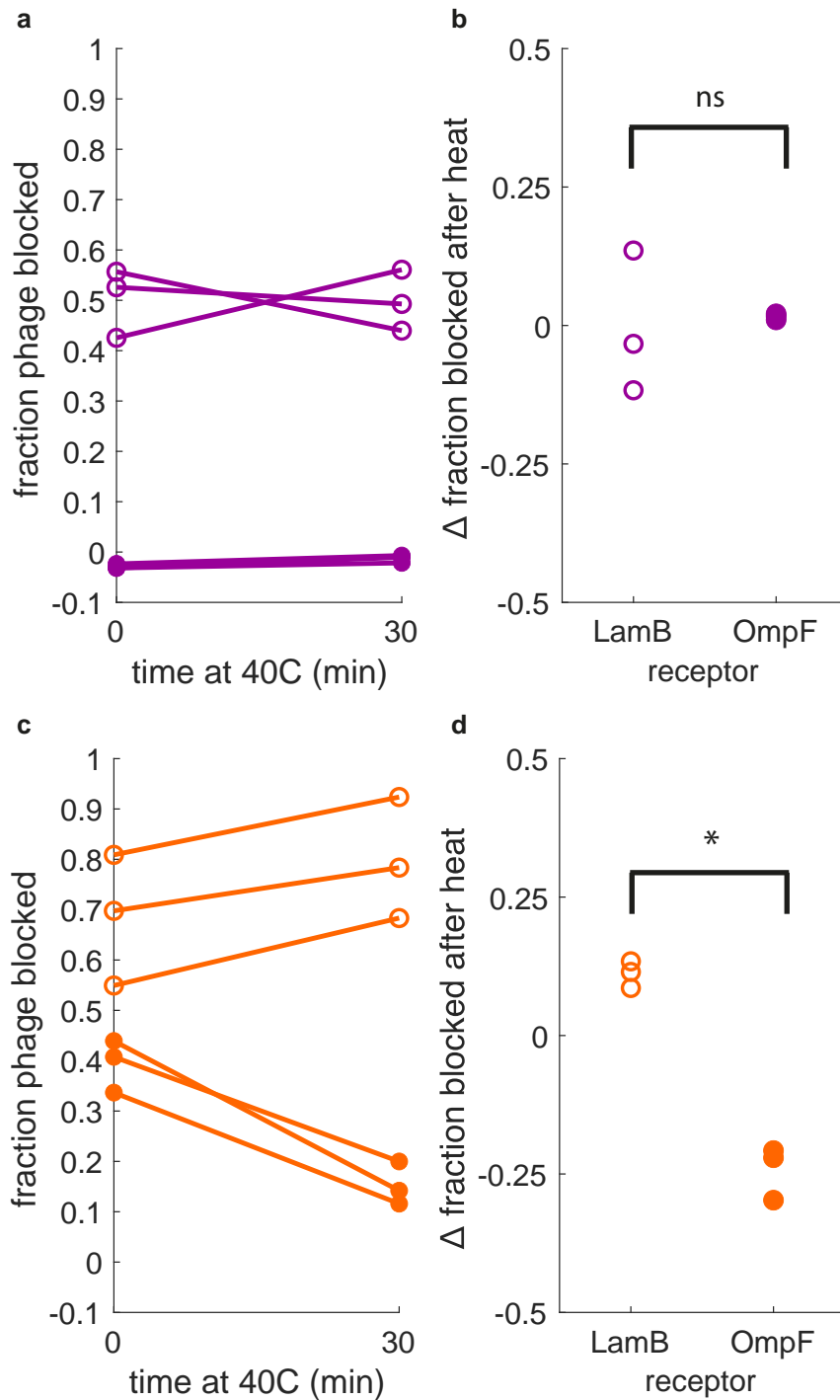


Fig. 4. A mild heat treatment selectively reduces activity on the new receptor, while not affecting activity on the ancestral receptor. This supports the hypothesis that an alternative, less stable conformation is responsible for binding the new receptor. Activity was measured indirectly by quantifying the fraction of phage blocked by preincubating cells with J protein prior to phage adsorption. Higher values on the y axis correspond to higher fraction of phage blocked from adsorbing, indicating higher J protein activity. Open circles correspond to measurements on the LamB receptor; closed circles correspond to measurements on the OmpF receptor. a) Activity of ancestor J protein on each receptor before and after heat treatment (heat treatment is indicated on x axis). Note that the ancestor J protein has activity only on LamB, as expected. b) Change in fraction blocked after heat treatment. The effect of the heat treatment on activity was indistinguishable between the two receptors (paired t -test, $t_{\text{stat}} = -0.2777$, $df = 2$, $P = 0.8073$). c) Activity of evolved J protein on each receptor before and after heat treatment (heat treatment is indicated on x axis). Note that the evolved J protein has activity on both LamB and OmpF, as expected. Activity of the evolved J protein on OmpF is reduced by the mild heat treatment, and activity on LamB is subtly increased. d) The effect of the heat treatment on activity was significantly different between LamB and OmpF receptors (paired t -test, $t_{\text{stat}} = 10.326$, $df = 2$, $P = 0.0092$). Bonferroni-adjusted significance values: ns = $P > 0.025$; * = $P < 0.025$.

initially triggered only by temperature, could become genetically encoded via selection over many generations (Waddington 1953). After selection, flies from lineages that experienced positive selection for the new phenotype expressed that phenotype regardless of temperature. Half a century later, West-Eberhard (2003) compiled extensive evidence from across diverse biological systems suggesting that nongenetic phenotypic variation resulting from differences in development can provide fuel for natural selection. New examples of organisms crossing evolutionary transitions by way of nongenetic phenotypic variation are still being discovered in diverse taxa, and modern methods are facilitating a deeper understanding of the genetics underpinning such transitions (Walworth et al. 2016; Signore and Storz 2020; Vigne et al. 2021). Our work adds to a growing body of research suggesting that this phenomenon may extend even to the evolution of RNA structures (Rezazadegan and Reidys 2018) and protein structures (Yadid et al. 2010; Sakuma et al. 2023).

A better understanding of the interaction between destabilizing mutations, protein metamorphosis, and evolvability could help shed light on the question of how proteins land on innovations among astronomically vast sequence space (Wagner 2014). The prevailing hypothesis is that neutral mutations create pathways in sequence space that allow proteins to change much of their sequence without deleterious costs, thereby placing them within a few mutations of an innovation (Wagner 2012). An alternative hypothesis is that sampling multiple phenotypes from the same genotype could allow proteins to reach new innovations more rapidly by relaxing the need for mutation (James and Tawfik 2003; Tokuriki and Tawfik 2009). If an expanded conformational repertoire can be achieved through generically destabilizing mutations rather than mutations that alter its shape in a highly specific way (Sikosek and Chan 2014), then innovations might be achieved rapidly because destabilizing mutations are common (Tokuriki et al. 2008). Prior work on the λ RBD suggested that mutational pathways leading to OmpF^+ require two types of mutations: a destabilizing mutation that generates structural heterogeneity, plus a loop mutation that fine-tunes the binding surface (Strobel et al. 2022). The findings of the present study provide the mechanism for how destabilizing mutations generate heterogeneity by interfering with the self-association of RBD monomers.

Our results might also help to guide efforts aiming to employ synthetic biology and directed evolution to generate proteins with novel functions. It is commonly suggested that directed evolution experiments intentionally stabilize proteins before or during rounds of mutagenesis and selection (Socha and Tokuriki 2013; Stimple et al. 2020). While there are certainly examples of increased stability improving outcomes of directed evolution experiments (Bloom and Arnold 2009), our results demonstrate how stabilizing a protein might cause the unintended outcome of reducing its ability to generate

conformational diversity and therefore reducing innovative capacity.

This study represents a step forward in understanding the mechanism of protein innovation that fueled a viral host-range expansion. We showed that phenotypic heterogeneity among whole λ particles that had evolved to use a new receptor in the previous study was likely caused by conformational heterogeneity in the RBP. This suggests that destabilization was not simply a deleterious cost of adaptation but instead had an independent evolutionary benefit of increasing conformational heterogeneity and potentiating OmpF^+ evolution. The role of protein heterogeneity in mediating evolutionary transitions is a growing area of interest, and our results suggest that virus host shifts can occur through this mechanism.

Materials and Methods

Media Recipes for Growing Bacteria and Phage

We prepared media used for culturing bacteria and phage following recipes published in Strobel et al. (2022).

Protein Constructs

For each protein variant (wild-type and evolved), two sets of constructs were purified. In one set, the 249 amino acid J domain was fused to MBP coding sequence via a short linker sequence that included a 6-histidine tag. These constructs were used in the functional heterogeneity assay in Fig. 3. To create these constructs, we used the In-Fusion Cloning Kit (Takara Bio), using the pMAL-c2x plasmid as a backbone. To generate the insert (composed of the 6-histidine tag plus the 249 amino acids of J), we first cloned the 249 amino acids of J into the pET-45b plasmid backbone, which contained the 6-histidine tag (oligos to linearize pET-45b: 5' CTTGTCGTCGTCATCATTCGAACC GGTACC and 5' AGTCCGGATCCCAATTGGGAGCTCG TG; and oligos to amplify the insert: 5' ATGGGATCC GGACTTCAGACCACGCTGATGCC and 5' GATGACGAC GACAAGATGGAGGACACGGAGGAAGG). We then amplified the 6-histidine tag + 249 amino acids of J from those constructs and cloned them into the pMAL-c2x backbone (oligos to linearize pMAL-c2x: 5' GAATTCTGAA ATCCTTCCCTCGATC and 5' AAGCTTGGCACTGGCC GTC; and oligos to amplify the insert: 5'-GGGAAGGA TTTCAGAATTCATGGCACATCACCACCAC and GCCAG TGCCAAGCTTTCAGACCACGCTGATGCCC). We transformed cloning products into Stellar Competent Cells (Takara Bio cat # 636767) and used colony PCR to verify the correct sequence (oligos: 5' TGGCGAAAGAT CCACGTATTG and 5' AGGCGATTAAGTTGGGTAACG). We then miniprep the plasmid and transformed it into BL21DE3 cells that we had modified to be *malT*⁻. The purpose of knocking out *malT* was to prevent the binding of expressed J proteins to LamB receptors on the outer membrane after cell lysis (*malT* regulates the expression of LamB, the receptor for the J protein; Chaudhry et al. 2018).

The second set of constructs contained only the 6-histidine tag and the C-terminal 152 C-terminal amino acids. These constructs were used in the thermal shift assay. To create these constructs, we used the Q5 site-directed mutagenesis kit (NEB catalog #E0554S, with oligos: 5' AACTGTACGATAAACGGTAC and CTTGTCTCGTCATCATTC) to delete the first 97 amino acids of J from constructs that had been previously generated containing the 249 C-terminal amino acids of J inserted in the pET-45b backbone. We transformed the products into NEB 5-alpha competent *Escherichia coli* and used colony PCR to screen for successful deletions (5' GCGAAATTA

ATACGACTCACTATA and 5' AAGGGTTATGCTAGTTATTG). We then minipreped the plasmid and transformed it into BL21DE3 cells that we had modified to be *malT*⁻.

Early in the project, we attempted to express a construct containing the full-length J protein, 1,132 amino acids, plus a 6-histidine tag, but it was completely insoluble, consistent with a previous study (Wang et al. 1998).

Protein Expression and Purification

To express proteins, we added 2-mL overnight BL21DE3 *malT*⁻ cultures containing the plasmid in 100-mL Luria Broth Lennox (LB) and 240- μ L 50-mg/mL carbenicillin for 2 h at 37 °C, shaking at 110 rpm. We then added 100 μ L of 1 M IPTG and incubated at room temperature (~22 °C), shaking at 110 rpm for 18 to 20 h. Expression cultures were then pelleted by centrifugation at 3,214 \times g for 10 min, resuspended in 10 mL of buffer containing 20 mM Tris-HCl pH 9.0 and 150 mM NaCl using an 18-gauge needle to reduce viscosity, and frozen at -80 °C for 30 min or overnight. Then, samples were thawed and sonicated in three cycles of 60 s at 20% amplitude, with 60 s on ice in between each round using a Fisher FB-50 sonic dismembrator with the standard 1/8" diameter microtip. Sonicates were centrifuged again at 3,214 \times g for 10 min at 10 °C, and the soluble fraction was collected by filtering supernatants through 0.22- μ m syringe filters.

Filtered supernatants were purified using 400 μ L of resuspended Ni-NTA resin (Thermo Scientific cat # 88221), using the batch method in 15-mL falcon tubes. The resin was first centrifuged at 500 \times g for 2 min and storage fluid was removed, and then the resin was washed with 4 mL of 20 mM Tris-HCl pH 9.0 and 150 mM NaCl, centrifuged again at 500 \times g for 2 min, and buffer removed. Then, 10 mL of sonicate was added to the washed resin and incubated for 30 min with periodic mixing. Then, the sample was centrifuged at 500 \times g for 2 min, and the supernatant was removed and discarded. The resin with bound protein was then washed four times using 4 mL of 20 mM Tris-HCl pH 9.0, 150 mM NaCl, and 20 or 80 mM imidazole (20 mM for the MBP-containing constructs and 80 mM for the MBP-free constructs). After the final wash, bound proteins were eluted from the resin using 20 mM Tris-HCl pH 9.0,

150 mM NaCl, and 380 mM imidazole and filtered through 0.22- μ m spin column filters.

SDS-PAGE

Samples were prepared for SDS-PAGE by combining 100- μ L sample with 100- μ L sample buffer (900- μ L 2 \times Laemmli sample buffer, Bio-Rad cat #1610737 + 100- μ L 1 M DTT), heating to 65 °C for 10 min, centrifuging at 16,000 \times g for 10 min, and loading 20 μ L in a 12% TGX gel (Bio-Rad cat #4561043).

Melting Point Determination Using Thermal Shift Assay

Purified protein samples of the MBP-free constructs were used for the thermal shift assays. Our protocol was designed following the current best practices in the field (Huynh and Partch 2015; Kazlauskas et al. 2021). First, the 5000 \times SYPRO Orange (Sigma-Aldrich catalog #S5692-50UL) was diluted to 200 \times in 20 mM Tris-HCl pH 9.0 and 150 mM NaCl. Then, three replicate wells of 45 μ L of protein sample and 5- μ L 200 \times SYPRO Orange were prepared for each protein variant in an optically clear PCR plate, covered with a clear adhesive seal. Three replicate controls were also run using elution buffer (20 mM Tris-HCl pH 9.0, 150 mM NaCl, and 380 mM imidazole) instead of the protein sample. Then, the sample was run on a Bio-Rad CFX96 qPCR machine with scan mode set to FRET, under the following thermal conditions: 25 °C for 15 min, followed by 0.5 °C incremental increase from 25 °C to 90 °C holding at each temperature for 30 s and then capturing a reading at each temperature step, followed by a final step at 25 °C for 5 min.

AlphaFold Structure Predictions

We generated structural predictions of our constructs using the publicly available version (Mirdita et al. 2022) of AlphaFold (Jumper et al. 2021) using all standard presets. We used the Foldseek server (Kempen et al. 2023) to identify structural similarity between predicted structures of J and known structures of viral tail spike proteins. We used PyMOL (Schrodinger Inc.) and Chimera (Pettersen et al. 2004) to visualize predicted structures.

Size exclusion chromatography coupled to multi-angle light scattering

For analysis of oligomeric states by SEC-MALS, a 100- μ L protein sample at 5 mg/mL was passed over a Superdex 200 10/300 GL column (Cytiva) in a buffer containing 20 mM Tris-HCl pH 7.5, 250 mM NaCl, 2 mM beta-mercaptoethanol, and 1 mM sodium azide. Light scattering and differential refractive index profiles were collected by miniDAWN TREOS and Optilab T-rEX detectors (Wyatt Technology), respectively, and molecular weight was calculated using ASTRA v.8 software (Wyatt Technology).

Functional Heterogeneity Assay

Purified MBP-containing constructs were used for this assay. Purified samples were first diluted to approximately 5 μ M and separated into three replicates of 800 μ L in Lo-Bind microcentrifuge tubes. Then, from each tube, 400 μ L was immediately sampled and set on ice (the preheat-treated sample). Samples were then incubated in a warm water bath at 40 °C for 30 min, and another 400 μ L was sampled and put on ice. The heated samples were filtered through 0.22- μ m spin column filters to remove any large aggregates.

Then, we measured the activity of each construct on each receptor, before and after heat treatment. We measured activity on receptors as a function of their ability to block receptors from being bound by whole phage particles. To measure this, we first incubated 100 μ L of 5 μ M protein with 10- μ L overnight bacteria culture ($\sim 10^7$ cells) expressing only LamB or only OmpF (Keio collection knockouts) (Baba et al. 2006) allowing the proteins to adsorb to the receptors on the cell surface. Then, we added whole phage particles and allowed the phage to adsorb to receptors not blocked by protein. Tubes were then placed on ice and centrifuged at 16,000 $\times g$ for 1 min, and 50 μ L of the supernatant (containing unbound phage) was plated with 100 μ L of wild-type *E. coli* (Keio collection parental strain BW25113) (Baba et al. 2006). For the whole phage particles, we chose a receptor generalist genotype of λ that can infect through both LamB and OmpF (Meyer et al. 2012). EvoC phage was induced from a lysogenic prophage integrated into the HWEC106 genome by heat shock (lysogen construction reported in Meyer 2016). Lysogens were grown up at 37 °C in LB, and then 140 μ L was inoculated into 4-mL LBM9 and 40- μ L MgSO₄, grown at 30 °C for 2 h, heat shocked at 42 °C for 15 min, and then incubated at 37 °C for 90 min. The lysate was filtered through a 0.22- μ m syringe filter and diluted in 9-mL M9 minimal media containing no sugar source, supplemented with 90- μ L MgSO₄.

We also included three replicate controls containing phage with LB media instead of cells and 20 mM Tris-HCl pH 9.0, 150 mM NaCl, and 380 mM imidazole buffer instead of protein, to calculate the total number of phages particles. Additionally, to capture the fraction of phage that adsorbs in the absence of protein, we included three replicate controls containing phage with LamB-only cells and 20 mM Tris-HCl pH 9.0, 150 mM NaCl, and 380 mM imidazole buffer instead of protein, as well as three analogous replicates with OmpF-only cells. Only about 1% to 2% of total phage remained unadsorbed to either cell type. To calculate the fraction of phage blocked by protein, we subtracted the number of unbound phages in the buffer treatment from the number of unbound phages in the protein treatment and divided the result by the total number of phages initially added.

To compare the effect of heat treatment on different receptors, we used a paired *t*-test. Because the variances were unequal for measurements on the ancestor protein,

an unequal variance *t*-test was also performed, and the significance did not change.

Acknowledgments

We thank Dr. Katherine Petrie for her valuable help and advice with this project. We thank Dr. Randolph Hampton, Dr. Sonya Neal, and Dr. Matthew Flagg for generously offering their expert advice and laboratory space for this project.

Funding

Funding for this project was provided by the Howard Hughes Medical Institute Emerging Pathogens Initiative.

Data Availability

All data are available at Dryad (datadryad.org): <https://doi.org/10.5061/dryad.pnvx0k6wn>.

References

- Baba T, Ara T, Hasegawa M, Takai Y, Okumura Y, Baba M, Datsenko K, Tomita M, Wanner B, Mori H. Construction of *Escherichia coli* K-12 in-frame, single-gene knockout mutants: the Keio collection. *Mol Syst Biol*. 2006;2(1):2006.0008. <https://doi.org/10.1038/msb4100050>.
- Berkane E, Orlik F, Stegmeier J, Charbit A, Winterhalter M, Benz R. Interaction of bacteriophage lambda with its cell surface receptor: an in vitro study of binding of the viral tail protein gpJ to LamB (Maltoporin). *Biochemistry*. 2006;45(8):2708–2720. <https://doi.org/10.1021/bi051800v>.
- Beveridge R, Migas L, Payne K, Nigel S, David L, Barran P. Mass spectrometry locates local and allosteric conformational changes that occur on cofactor binding. *Nat Commun*. 2016;7(1):12163. <https://doi.org/10.1038/ncomms12163>.
- Bloom JD, Arnold FH. In the light of directed evolution: pathways of adaptive protein evolution. *Proc Natl Acad Sci U S A*. 2009;106(supplement_1):9995–10000. <https://doi.org/10.1073/pnas.0901522106>.
- Bloom JD, Labthavikul ST, Otey CR, Arnold FH. Protein stability promotes evolvability. *Proc Natl Acad Sci U S A*. 2006;103(15):5869–5874. <https://doi.org/10.1073/pnas.0510098103>.
- Boon M, Holtappels D, Lood C, van Noort V, Lavigne R. Host range expansion of *Pseudomonas* virus LUZ7 is driven by a conserved tail fiber mutation. *PHAGE*. 2020;1(2):87–90. <https://doi.org/10.1089/phage.2020.0006>.
- Carr C, Kim P. A spring-loaded mechanism for the conformational change of influenza hemagglutinin. *Cell*. 1993;73(4):823–832. [https://doi.org/10.1016/0092-8674\(93\)90260-W](https://doi.org/10.1016/0092-8674(93)90260-W).
- Chang Y, Cohen Y, Phong C, Myers W, Kim Y, Tseng R, Lin J, Zhang L, Boyd J, Lee Y, et al. A protein fold switch joins the circadian oscillator to clock output in cyanobacteria. *Science*. 2015;349(6245):324–328. <https://doi.org/10.1126/science.1260031>.
- Chaudhry W, Pleška M, Shah N, Weiss H, McCall I, Meyer J, Gupta A, Guet C, Levin B. Leaky resistance and the conditions for the existence of lytic bacteriophage. *PLoS Biol*. 2018;16(8):e2005971. <https://doi.org/10.1371/journal.pbio.2005971>.
- Crowther G, He P, Rodenbough P, Thomas A, Kovzun K, Leibly D, Bhandari J, Castaneda L, Hol W, Gelb M, et al. Use of thermal melt curves to assess the quality of enzyme preparations. *Anal*

- Biochem.* 2010;**399**(2):268–275. <https://doi.org/10.1016/j.ab.2009.12.018>.
- Cuevas JM, Moya A, Sanjuán R. A genetic background with low mutational robustness is associated with increased adaptability to a novel host in an RNA virus. *J Evol Biol.* 2009;**22**(10):2041–2048. <https://doi.org/10.1111/j.1420-9101.2009.01817.x>.
- Dellus-Gur E, Elias M, Caselli E, Prati F, Salverda M, de Visser J, Fraser J, Tawfik D. Negative epistasis and evolvability in TEM-1 β -lactamase—the thin line between an enzyme’s conformational freedom and disorder. *J Mol Biol.* 2015;**427**(14):2396–2409. <https://doi.org/10.1016/j.jmb.2015.05.011>.
- Dishman A, Volkman B. Unfolding the mysteries of protein metamorphosis. *ACS Chem Biol.* 2018;**13**(6):1438–1446. <https://doi.org/10.1021/acscchembio.8b00276>.
- Huynh K, Partch C. Analysis of protein stability and ligand interactions by thermal shift assay. *Curr Protoc Protein Sci.* 2015;**79**(1):28.9.1–28.9.14. <https://doi.org/10.1002/0471140864.ps2809s79>.
- Kempen M, Kim SS, Tumescheit C, Mirdita M, Lee J, Gilchrist CLM, Soding J, Steinegger M. Fast and accurate protein structure search with Foldseek. *Nat Biotechnol.* 2023;**42**(2):243–246. <https://doi.org/10.1038/s41587-023-01773-0>.
- James L, Tawfik D. Conformational diversity and protein evolution—a 60-year-old hypothesis revisited. *Trends Biochem Sci.* 2003;**28**(7):361–368. [https://doi.org/10.1016/S0968-0004\(03\)00135-X](https://doi.org/10.1016/S0968-0004(03)00135-X).
- Jumper J, Evans R, Pritzel A, Green T, Figurnov M, Ronneberger O, Tunyasuvunakool K, Bates R, Židek A, Potapenko A, et al. Highly accurate protein structure prediction with AlphaFold. *Nature.* 2021;**596**(7873):583–589. <https://doi.org/10.1038/s41586-021-03819-2>.
- Kazlauskas E, Petrauskas V, Paketurytė V, Matulis D. Standard operating procedure for fluorescent thermal shift assay (FTSA) for determination of protein–ligand binding and protein stability. *Eur Biophys J.* 2021;**50**(3–4):373–379. <https://doi.org/10.1007/s00249-021-01537-1>.
- Li J, Browning S, Mahal SP, Oelschlegel AM, Weissmann C. Darwinian evolution of prions in cell culture. *Science.* 2009;**327**(5967):869–872. <https://doi.org/10.1126/science.1183218>.
- Luo X, Yu H. Protein metamorphosis: the two-state behavior of Mad2. *Structure.* 2008;**16**(11):1616–1625. <https://doi.org/10.1016/j.str.2008.10.002>.
- Madhurima K, Nandi B, Sekhar A. Metamorphic proteins: the Janus proteins of structural biology. *Open Biol.* 2021;**11**(4):210012. <https://doi.org/10.1098/rsob.210012>.
- Markley J, Kim J, Dai Z, Bothe J, Cai K, Frederick R, Tonelli M. Metamorphic protein IscU alternates conformations in the course of its role as the scaffold protein for iron-sulfur cluster biosynthesis and delivery. *FEBS Lett.* 2013;**587**(8):1172–1179. <https://doi.org/10.1016/j.febslet.2013.01.003>.
- Meyer JR, Dobias DT, Medina SJ, Servilio L, Gupta A, Lenski RE. Ecological speciation of bacteriophage lambda in allopatry and sympatry. *Science.* 2016;**354**(6317):1301–1304. <https://doi.org/10.1126/science.aai8446>.
- Meyer JR, Dobias DT, Weitz JS, Barrick JE, Quick RT, Lenski RE. Repeatability and contingency in the evolution of a key innovation in phage lambda. *Science.* 2012;**335**(6067):428–432. <https://doi.org/10.1126/science.1214449>.
- Mirdita M, Schütze K, Moriawaki Y, Heo L, Ovchinnikov S, Steinegger M. ColabFold—making protein folding accessible to all. *Nat Methods.* 2022;**19**(6):679–682. <https://doi.org/10.1038/s41592-022-01488-1>.
- Nallamsetty S, Austin B, Penrose K, Waugh D. Gateway vectors for the production of combinatorially-tagged His6-MBP fusion proteins in the cytoplasm and periplasm of *Escherichia coli*. *Protein Sci.* 2005;**14**(12):2964–2971. <https://doi.org/10.1110/ps.051718605>.
- Oldfield C, Dunker A. Intrinsically disordered proteins and intrinsically disordered protein regions. *Annu Rev Biochem.* 2014;**83**(1):553–584. <https://doi.org/10.1146/annurev-biochem-072711-164947>.
- Petrie KL, Palmer ND, Johnson DT, Medina SJ, Yan SJ, Li V, Burmeister AR, Meyer JR. Destabilizing mutations encode nongenetic variation that drives evolutionary innovation. *Science.* 2018;**359**(6383):1542–1545. <https://doi.org/10.1126/science.aar1954>.
- Pettersen E, Goddard T, Huang C, Couch G, Greenblatt D, Meng E, Ferrin T. UCSF chimera—a visualization system for exploratory research and analysis. *J Comput Chem.* 2004;**25**(13):1605–1612. <https://doi.org/10.1002/jcc.20084>.
- Rezazadegan R, Reidys C. Degeneracy and genetic assimilation in RNA evolution. *BMC Bioinformatics.* 2018;**19**(1):543. <https://doi.org/10.1186/s12859-018-2497-3>.
- Roche S, Rey F, Gaudin Y, Bressanelli S. Structure of the prefusion form of the vesicular stomatitis virus glycoprotein G. *Science.* 2007;**315**(5813):843–848. <https://doi.org/10.1126/science.1135710>.
- Russell CJ. Hemagglutinin stability and its impact on influenza A virus infectivity, pathogenicity, and transmissibility in avians, mice, swine, seals, ferrets, and humans. *Viruses.* 2021;**13**(5):746. <https://doi.org/10.3390/v13050746>.
- Sakuma M, Honda S, Ueno H, Tabata KV, Miyazaki K, Tokuriki N, Noji H. Genetic perturbation alters functional substates in alkaline phosphatase. *J Am Chem Soc.* 2023;**145**(5):2806–2814. <https://doi.org/10.1021/jacs.2c06693>.
- Signore AV, Storz JF. Biochemical pedomorphosis and genetic assimilation in the hypoxia adaptation of Tibetan antelope. *Sci Adv.* 2020;**6**(25):eabb5447. <https://doi.org/10.1126/sciadv.abb5447>.
- Sikosek T, Chan HS. Biophysics of protein evolution and evolutionary protein biophysics. *J R Soc Interface.* 2014;**11**(100):20140419. <https://doi.org/10.1098/rsif.2014.0419>.
- Sinclair JF, Ziegler MM, Baldwin TO. Kinetic partitioning during protein folding yields multiple native states. *Nat Struct Biol.* 2022;**1**(5):320–326. <https://doi.org/10.1038/nsb0594-320>.
- Socha R, Tokuriki N. Modulating protein stability—directed evolution strategies for improved protein function. *FEBS J.* 2013;**280**(22):5582–5595. <https://doi.org/10.1111/febs.12354>.
- Stimple S, Smith M, Tessier P. Directed evolution methods for overcoming trade-offs between protein activity and stability. *AIChE J.* 2020;**66**(3):e16814. <https://doi.org/10.1002/aic.16814>.
- Strobel H, Horwitz E, Meyer J. Viral protein instability enhances host-range evolvability. *PLoS Genet.* 2022;**18**(2):e1010030. <https://doi.org/10.1371/journal.pgen.1010030>.
- Studer RA, Christin PA, Williams MA, Orengo CA. Stability-activity tradeoffs constrain the adaptive evolution of RubisCO. *Proc Natl Acad Sci U S A.* 2014;**111**(6):2223–2228. <https://doi.org/10.1073/pnas.1310811111>.
- Tokuriki N, Stricher F, Serrano L, Tawfik DS. How protein stability and new functions trade off. *PLoS Comput Biol.* 2008;**4**(2):e1000002. <https://doi.org/10.1371/journal.pcbi.1000002>.
- Tokuriki N, Tawfik DS. Protein dynamism and evolvability. *Science.* 2009;**324**(5924):203–207. <https://doi.org/10.1126/science.1169375>.
- Tuinstra R, Peterson F, Kutlesa S, Elgin E, Kron M, Volkman B. Interconversion between two unrelated protein folds in the lymphotactin native state. *Proc Natl Acad Sci U S A.* 2008;**105**(13):5057–5062. <https://doi.org/10.1073/pnas.0709518105>.
- Tétart F, Repoila F, Monod C, Krisch H. Bacteriophage T4 host range is expanded by duplications of a small domain of the tail fiber adhesin. *J Mol Biol.* 1996;**258**(5):726–731. <https://doi.org/10.1006/jmbi.1996.0281>.
- Vigne P, Gimond C, Ferrari C, Vielle A, Hallin J, Pino-Querido A, El Mouridi S, Mignerot L, Frøkjær-Jensen C, Boulin T, et al. A single-nucleotide change underlies the genetic assimilation of a plastic trait. *Science.* 2021;**7**:eabd9941. <https://doi.org/10.1126/sciadv.abd9941>.

- Waddington CH. Genetic assimilation of an acquired character. *Evolution*. 1953;**7**(2):118–126. <https://doi.org/10.2307/2405747>.
- Wagner A. The role of robustness in phenotypic adaptation and innovation. *Proc Biol Sci*. 2012;**279**(1732):1249–1258. <https://doi.org/10.1098/rspb.2011.2293>.
- Wagner A. *Arrival of the fittest*. New York (New York): Current; 2014.
- Walworth NG, Lee MD, Fu F-X, Hutchins DA, Webb EA. Molecular and physiological evidence of genetic assimilation to high CO₂ in the marine nitrogen fixer *Trichodesmium*. *Proc Natl Acad Sci U S A*. 2016;**113**(47):E7367–E7374. <https://doi.org/10.1073/pnas.1605202113>.
- Wang J, Hofnung M, Charbit A. The C-terminal portion of the tail fiber protein of bacteriophage lambda is responsible for binding to Lamb, its receptor at the surface of *Escherichia coli* K-12. *J Bacteriol*. 2000;**182**(2):508–512. <https://doi.org/10.1128/JB.182.2.508-512.2000>.
- Wang J, Michel V, Hofnung M, Charbit A. Cloning of the J gene of bacteriophage lambda, expression and solubilization of the J protein: first in vitro studies on the interactions between J and Lamb, its cell surface receptor. *Res Microbiol*. 1998;**149**(9):611–624. [https://doi.org/10.1016/S0923-2508\(99\)80009-6](https://doi.org/10.1016/S0923-2508(99)80009-6).
- Wang X, Minasov G, Shoichet BK. Evolution of an antibiotic resistance enzyme constrained by stability and activity trade-offs. *J Mol Biol*. 2002;**320**(1):85–95. [https://doi.org/10.1016/S0022-2836\(02\)00400-X](https://doi.org/10.1016/S0022-2836(02)00400-X).
- West-Eberhard MJ. *Developmental plasticity and evolution*. New York (New York): Oxford University Press; 2003.
- Wong C, Duan J, Gu Z, Ge X, Zeng J, Wang J. Architecture of the bacteriophage lambda tail. *Structure*. 2024;**32**(1):35–46.e3. <https://doi.org/10.1016/j.str.2023.10.006>.
- Yadid I, Kirshenbaum N, Sharon M, Dym O, Tawfik DS. Metamorphic proteins mediate evolutionary transitions of structure. *Proc Natl Acad Sci U S A*. 2010;**107**(16):7287–7292. <https://doi.org/10.1073/pnas.0912616107>.
- Yehl K, Lemire S, Yang AC, Ando H, Mimeo M, Torres MT, de la Fuente-Nunez C, Lu TK. Engineering phage host-range and suppressing bacterial resistance through phage tail fiber mutagenesis. *Cell*. 2019;**179**(2):459–469.e9. <https://doi.org/10.1016/j.cell.2019.09.015>.